Structural Engineering and Mechanics, Vol. 40, No. 6 (2011) 867-883
DOI: http://dx.doi.org/10.12989/sem.2011.40.6.867

Behavior of exterior reinforced concrete beam-column joints including a new reinforcement

Matthew J. Fisher[1a] and Halil Sezen*[2]

[1]*URS Corporation, Cleveland, Ohio, USA*
[2]*Department of Civil and Environmental Engineering and Geodetic Science, The Ohio State University, Columbus, Ohio, USA*

(Received May 13, 2010, Revised February 28, 2011, Accepted November 7, 2011)

Abstract. Six reinforced concrete beam-column joint specimens were constructed and tested under reverse cyclic loading to failure. The six specimens were divided into three groups, each group representing a different joint design. The main objectives of this study are to investigate the response of joints with three different design, reinforcement detailing and beam strengths, and to evaluate and compare the responses of beam-column joints reinforced with traditional steel rebar and a recently proposed steel reinforcement called prefabricated cage system (PCS). Each of the three test specimen designs included equivalent amount of steel reinforcement and had virtually identical details. The results of the research show that the PCS reinforced joints had a slightly higher strength and significantly larger deformation capacity than the equivalent rebar reinforced joints.

Keywords: beam-column joints; steel reinforcement; reinforced concrete; shear failure

1. Introduction

Beam-column joints are one of the most critical components in reinforced concrete frame structures, especially if the structure is located in a high seismic region. Recent earthquakes have shown that failure of beam-column joints often leads to collapse of the entire building (Sezen *et al*. 2000, Dogangun 2004, Zhao *et al*. 2008). A complex combination of shear and flexural stresses acts simultaneously within the joint region. Design of a joint is often governed by shear forces which are transferred through the joint, along with the ability of the joint to remain intact under reverse-cyclic loading. Both of these conditions are directly correlated to the amount and detailing of the reinforcement present within the joint. Without proper reinforcement detailing and resulting confinement of concrete inside the joint region, the concrete cracks and spalls off, reducing the shear and axial capacity of the column while also allowing the tensile longitudinal reinforcing bars of the beams to slip out. In order to improve the seismic performance of joints, non-conventional reinforcement arrangements, details and materials have been investigated (Jiuru *et al*. 2992, Bakir 2003, Shannag *et al*. 2005, Gencoglu 2007, Bindhu *et al*. 2008). Similarly, this study investigates

*Corresponding author, Associate Professor, E-mail: sezen.1@osu.edu
[a]Structural Engineer

Fig. 1 Equivalent PCS reinforcement and rebar reinforcing cage

the effectiveness of a non-conventional reinforcement in the joint region.

Traditionally, reinforced concrete members consist of reinforcing bar (rebar) cages encased within concrete. Due to the fact that rebar has been used almost exclusively for many decades, extensive research has been dedicated to determine the strength and deformation capacity of beam-column joints (Bakir and Boduroglu 2002, Lee *et al*. 2009, Alemdar and Sezen 2010).

Recently, a new method for reinforcing concrete has been proposed by Sezen and Shamsai (2008) at the Ohio State University. The prefabricated cage system (PCS) reinforcement consists of a monolithic reinforcing cage constructed from a hollow steel tube with openings cut into it through laser-cutting (Fig. 1). A PCS reinforcing cage is a single unit which performs the functions of both longitudinal reinforcing bars and transverse reinforcing bars. PCS allows for more effectively confined core to maintain its strength once the concrete cracks and spalls off. Through quick and precise off-site fabrication of PCS reinforcement possible inaccuracies associated with the tying of conventional rebar cages can be avoided. In this research, PCS was produced by laser cutting (Fig. 1) to ensure the greatest accuracy. Detailed description and discussion of production, structural performance, and economic evaluation of PCS can be found elsewhere (Shamsai 2006, Shamsai *et al*. 2007, Sezen and Shamsai 2008, Sezen and Miller 2011). Based on the analysis of a case study building, Shamsai *et al*. (2007) concluded that the PCS results in significant time and cost savings, and PCS is more economical than rebar used in traditional reinforced concrete construction. Shamsai (2006) tested a total of 32, 457-mm tall by 152-mm square small-scale columns, of which 16 were constructed with normal strength concrete, and the rest were constructed with high strength concrete. It was found that PCS reinforcement generally increases the axial strength and deformation capacity of the columns.

PCS reinforcement allows inspection of concrete after the member is subjected to extreme loading conditions. It may be extremely difficult to inspect concrete inside concrete-lled tubular systems

(CFT) or possible deterioration of bond between the tube and concrete, for example after an earthquake. PCS also enables easy connection of reinforced concrete beam and column. Connection of reinforced concrete beams to a CFT column can be very difficult and labor intensive (Bai *et al*. 2008, Qu *et al*. 2009).

2. Experimental test program

A total of six exterior beam-column joint specimens were constructed and tested to investigate the effectiveness of different reinforcement details in the joint region. Specimens were divided into three groups, each with a distinct joint design. Specimens within a group were constructed from reinforcement with varying nominal yield strengths, however, the equivalent axial force capacity of steel (yield strength times cross sectional area) was kept constant. Test variables, excluding the method of reinforcement, included transverse reinforcement spacing and joint strength. Specimens were tested under quasi-static reverse cyclic loading until failure.

The joint design varied based on the amount of beam longitudinal steel or the ratio of beam flexural strength to column flexural strength and on the spacing of transverse reinforcement in the column and beam. The specimens were divided into three groups: the design group with a column flexural strength greater than the beam flexural strength (Group C), the design group with approximately equal beam and column flexural strengths (Group E), and the design group with a beam flexural strength greater than the column flexural strength (Group B). Each group contained two specimens: one with a rebar reinforced column, and one PCS reinforced column. A naming convention was developed for reference purposes. The first letter refers to the group that the specimen is in: C (column stronger than beam), E (equal strengths) and B (beam stronger than column). This is followed by a number, which corresponds to the joint type: 1 (non-seismic joint design) or 2 (seismic joint design). This is followed by an abbreviation referring to the type of column reinforcement used: RC (rebar) or PCS (PCS reinforcement).

All specimens were tested following the same pre-determined loading history, which was a function of yield strength of the beam in each group. The test was controlled using an MTS Flextest SE digital servo test controller. The load applied at the tip of the cantilever beam was recorded using an 89 kN load cell attached to the actuator. An upward tensile load at the end of the beam was considered positive, while a downward compressive load was considered negative during reverse-cyclic loading.

Fig. 2 shows details of the test setup and a specimen used in the experiments. The testing station was designed to restrain the top and bottom ends of the column. A steel angle was attached to the base plate at the top of the column to resist lateral forces. Threaded rods were positioned between the plate on top of the column and the plate below the column. These rods on each side of the column were placed into tension by tightening the nut above the top plate to apply the design compressive load onto the column. The tension force in the threaded rods, and equivalently the compressive force on the column, was calculated using the strains measured by strain gauges attached to the threaded rods. The rods were tensioned until the strain in the rods was approximately equal to 700×10^{-6}, which is equivalent to 71.2 kN of tension in each rod. This tension load in each rod translates to a 142.3 kN compression load on the column of the test specimen, which is approximately 15% of axial capacity of the column.

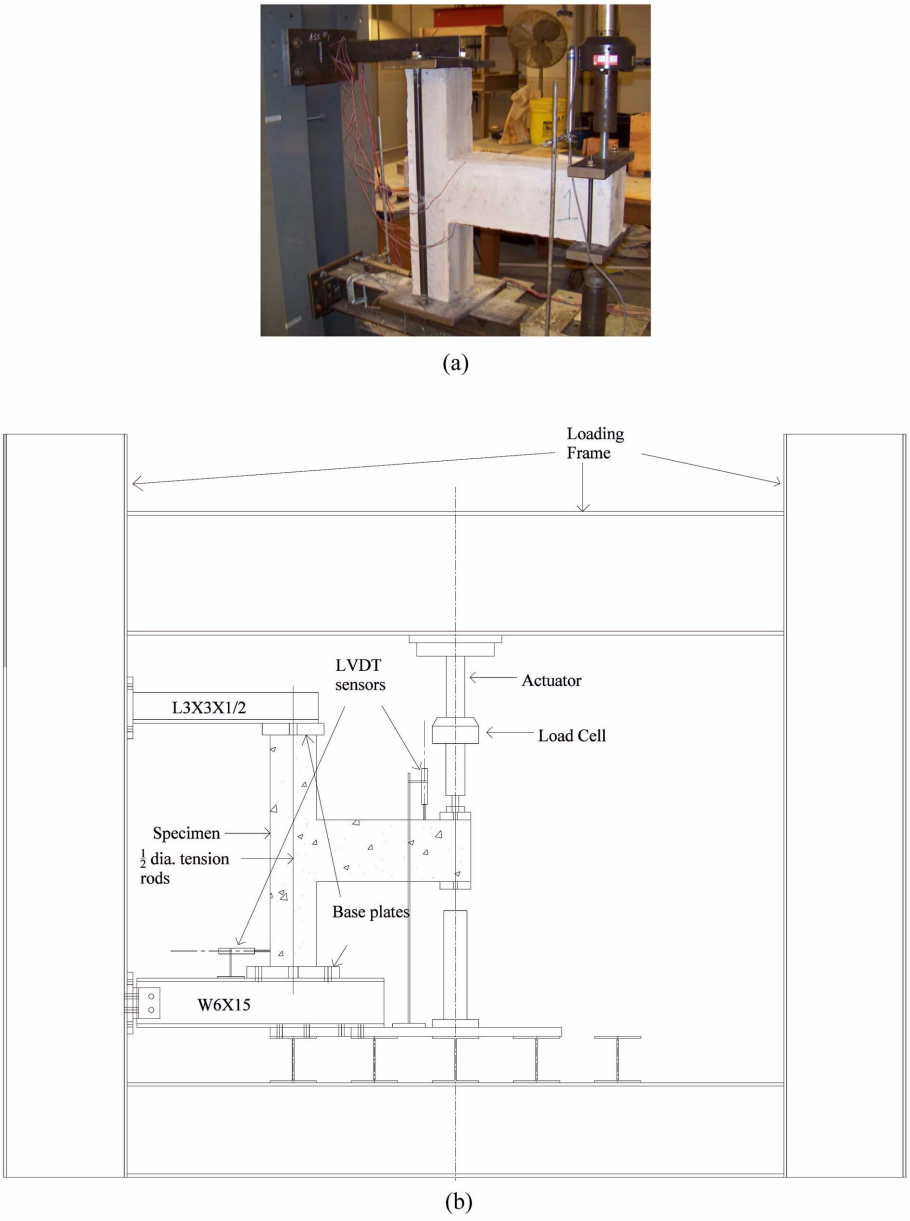

Fig. 2 Test setup and specimen

3. Specimen design, loading and instrumentation

The requirements of ACI 318 Building Code (2005) and ASCE-ACI 352 Committee Report (2002) were utilized in the design of specimens. While not all code requirements could be followed exactly, due to smaller scale of specimens, the design was able to meet almost all code requirements. The columns had 152 mm square sections, with a height of 762 mm. The beams were

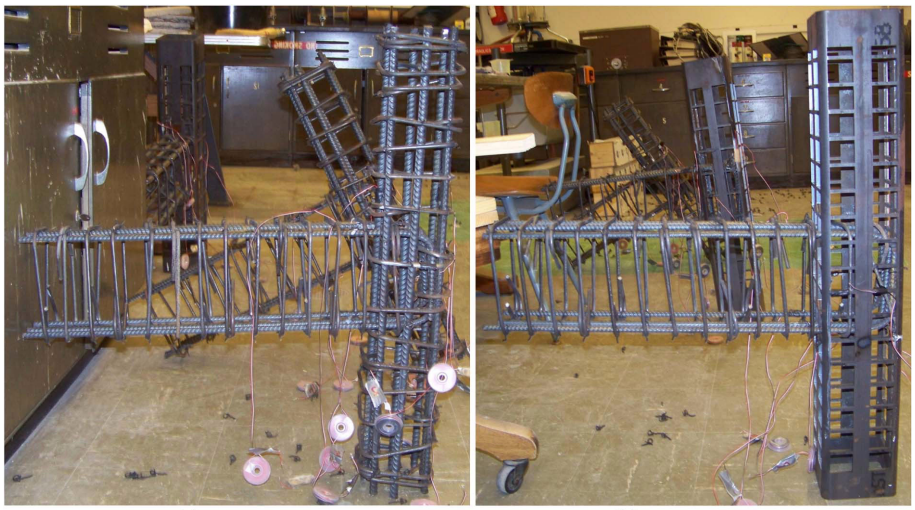

(a) (b)

Fig. 3 Reinforcement cages for specimens: (a) C-2-RC, and (b) C-2-PCS

152 mm wide and 203 mm deep with a length of 508 mm from the face of the column. The amount of longitudinal reinforcement was held constant for all six columns. Rebar reinforced columns had eight 12.7 mm diameter steel bars. An equivalent area of longitudinal steel provided in the PCS columns was calculated based on the ratio of the yield strengths of the rebar and PCS tube steel. The diameter of the transverse reinforcing bars was 6.4 mm. The spacing of the column ties and stirrups varied within groups based on design requirements. This design resulted in a column flexural strength of 24.7 kN-m in all specimens. The beams were all reinforced with three longitudinal bars on top and three bars on the bottom. 6.4 mm diameter bars were used for rectangular closed stirrups with 135 degree end hooks.

The specimens in Group C were designed according to the seismic requirements of the ACI 318 code (Chapter 21 of ACI 318-05). According to seismic code requirements, design strength of longitudinal tension rebar in the beam is taken equal to 1.25 times the yield strength of the rebar. ACI 318-05 seismic requirements also requires that the flexural strength of the columns, M_{nc} be at least 1.2 times the flexural strength, M_{nb} of beams framing into that column. The longitudinal beam reinforcement consisted of three 9.5 mm diameter bars on top and bottom. This resulted in a tensile steel ratio of 0.007 and a flexural strength, M_{nb}, of 18.1 kN-m. Reinforcement cages for Group C specimens are shown in Fig. 3.

The longitudinal reinforcement in the beams in Group E was designed such that the flexural strength of the beam was approximately equal to the flexural strength of the column. The final beam reinforcement consisted of two 12.7 mm diameter bars and one 9.5 mm diameter bar on top and bottom, respectively. This resulted in a flexural strength, M_{nb} of 22.0 kN-m. The final reinforcement in Group B beams consisted of three 12.7 mm diameter bars on top and bottom. This resulted in a tensile steel reinforcement ratio of 0.0125 and a flexural strength, M_{nb} of 25.5 kN-m.

The joint shear strength was calculated based on methods prescribed in ACI 352 (2002). The shear force in the column was calculated from Eq. (1) with the assumption that the ends of the test columns represent column inflection points in a building frame subjected to lateral earthquake loads.

$$V_{col} = \frac{M_n}{l_{pc}} \tag{1}$$

where V_{col} is the shear force in the column, M_n is the moment capacity of the beam, and l_{pc} is the distance between inflection points or the total column height of the specimen. Total shear force in the joint, V_u can be calculated from Eq. (2) as the summation of shear carried through the column and shear force resulting from the beam tensile reinforcement.

$$V_u = T_n - V_{col} \tag{2}$$

where T_n is equal to the tensile force in the beam longitudinal reinforcement, which can be calculated from Eq. (3). The shear strength of the joint is calculated in Eq. (4).

$$T_n = \alpha A_{st} f_y \tag{3}$$

$$\phi V_n = \phi \gamma \sqrt{f_c'} b_j h_c \tag{4}$$

where ϕ is the strength reduction factor, b_j is the effective joint width, h_c is the depth of the column in the direction of the shear, and γ is a factor based on the type of connection, which is provided in ACI 318 (2005). In this research, a strength reduction factor of 0.85 allowed by ACI 352 (2002) was used.

Summary of design calculations are presented in Table 1. It should be noted the specified material properties were used in design. The specified concrete strength was 28 MPa, and the specified yield strength of steel materials was 414 MPa. Same concrete was used in all specimens. An average compressive strength of 30 MPa was obtained from concrete cylinder tests. The measured yield

Table 1 Summary of specimen design parameters

Design description and parameters	Symbol (unit)	Group C	Group E	Group B
Joint type (ACI 352-02)		2	1	1
Area of beam tensile reinforcement	A_{sb} (cm^2)	2.1	3.3	3.9
Beam flexural strength (calculated, ACI 318-05)	M_{nb} (kN-m)	18.1	22.0	25.5
Beam stirrup spacing (provided, ACI 318-05)	s_b (cm)	3.8	8.9	4.4
Beam concrete shear strength (ACI 318-05)	V_{bc} (kN)	23.8	23.8	23.8
Beam steel shear strength (ACI 318-05)	V_{bs} (kN)	29.0	40.2	50.6
Column tie spacing (provided, ACI 318-05)	s_c (cm)	3.8	6.4	6.4
Column shear force (Equation 1)	V_{col} (kN)	23.8	28.8	33.5
Column concrete shear strength (ACI 318-05)	V_{cc} (kN)	24.4	24.4	24.4
Column steel shear strength (ACI 318)	V_{cs} (kN)	7.3	14.1	20.3
Tensile force in beam reinforcement (Equation 3)	T_n (kN)	110.1	136.1	160.1
Joint shear force (Equation 2)	V_u (kN)	86.3	107.2	126.8
Joint shear strength (Equation 4)	ϕV_n (kN)	103.2	129.0	129.0
Tensile reinforcement development length (ACI 318-05)	l_{dh} (cm)	14.0	13.5	13.5

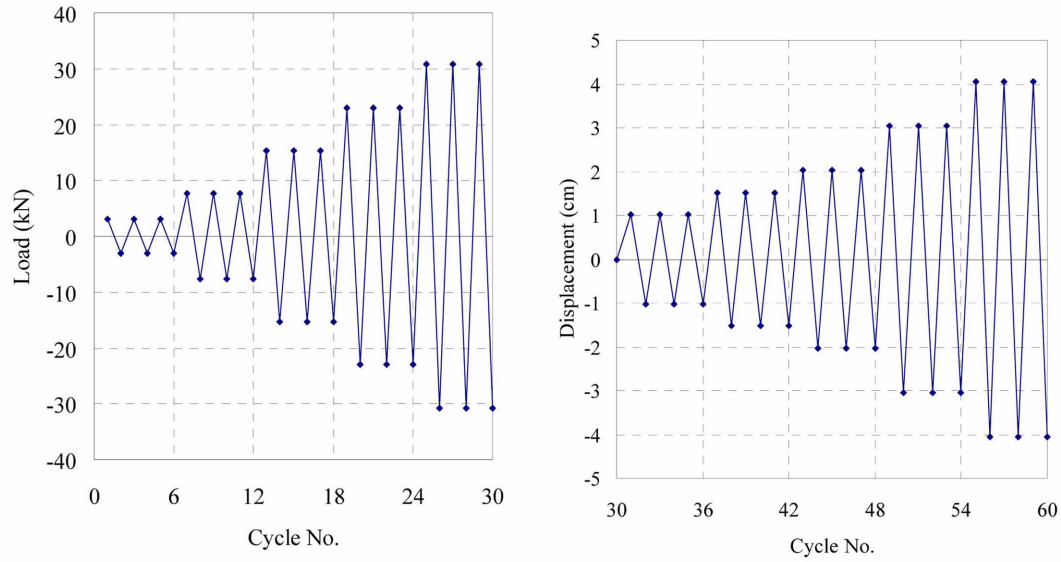

Fig. 4 Force controlled and displacement controlled loading histories for group C specimens

strengths of 6.4 mm diameter column ties and stirrups, 9.5 and 12.7 mm diameter deformed longitudinal bars, and 6.4 mm thick steel tube were 376, 493, 435, and 393 MPa, respectively.

Each specimen was subjected to monotonically increasing cyclic load applied at the tip of the cantilever beam. The experiments were force controlled until the yield strength of the beam (P_y) was reached. Beyond yield strength, loading was applied following a predetermined displacement controlled loading scheme. Each specimen was initially subjected to three cycles of loads at magnitudes P_y / 10, P_y / 4, P_y / 2, 3P_y / 4 and P_y. After yielding in the beam, theoretically at P_y, three cycles of loads at displacement magnitudes $2\Delta_y$, $3\Delta_y$, $4\Delta_y$, $6\Delta_y$ and $8\Delta_y$ were applied until the failure occurred. The yielding load, P_y was equal to 47.1, 30.7 and 54.5 kN for Group E, C and B specimens, respectively. Group B specimens failed at the end of force controlled cycles. The yield displacement, Δ_y was 17.8 mm and 5.1 mm for Group E and C specimens, respectively. As an example, the loading histories for specimens in Group C are shown in Fig. 4.

Strain gauges were attached on a select number of steel bars within the reinforcing cage in order to better understand the behavior of the joint. Type CEA-06-250UW-120 electrical resistance uni-directional strain gauges with a nominal resistance of 120 ohms were used. The actual locations of the strain gauges are shown in Fig. 5 and instrumentation details are provided in Fisher (2009). Two gauges were placed on the back face and the front face of the column reinforcement (SG #1, #2, #5 and #6 in Fig. 5 respectively), two gauges were placed on the lateral column tie located within the center of the joint (SG #3 and #4 in Fig. 5), and two gauges were placed on the beam reinforcement, one each on a top and bottom longitudinal bar located on the right side of the specimen (SG #7 and #8 in Fig. 5). Strain gauges were covered with an epoxy coating to protect them from concrete during casting of the specimens. A sample of a recorded load versus strain relationship is provided in Fig. 6. Deflections and strains measured in all specimens are provided in Fisher (2009).

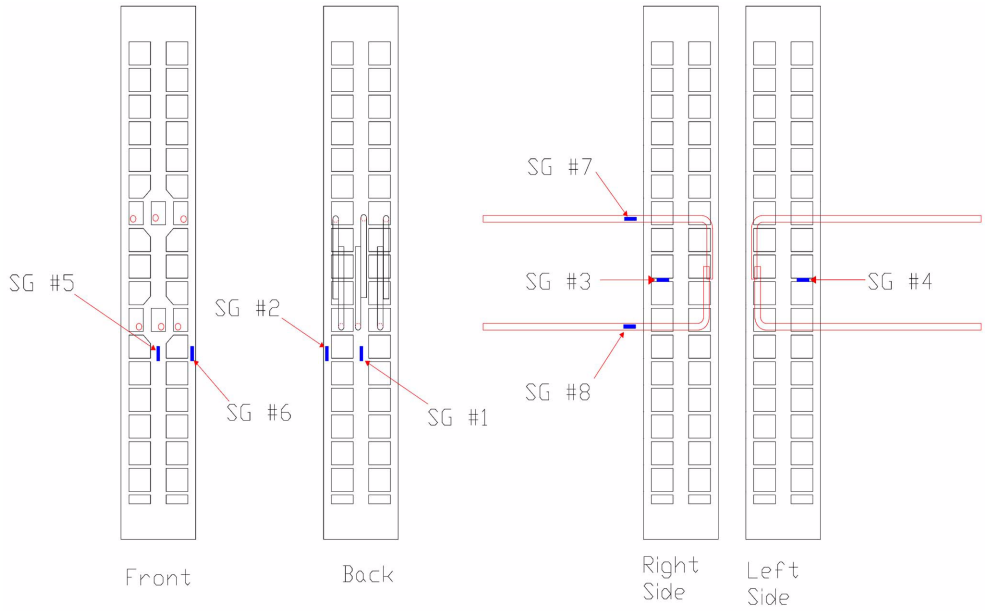

Fig. 5 Location of strain gauges on a typical reinforcing cage

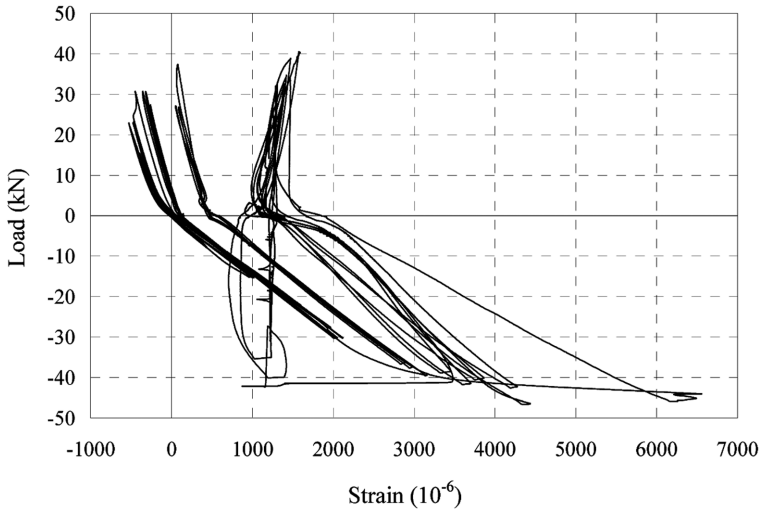

Fig. 6 Measured load versus strain relationship for gauge 8 on C-2-RC

4. Experimental results

The overall specimen behavior was similar within each respective group. Fig. 7 shows examples of a PCS and a rebar reinforced joint when they lost their load carrying capacity. The observed responses of specimens are discussed and compared below. Details of test results and failure modes can be found in Fisher (2009).

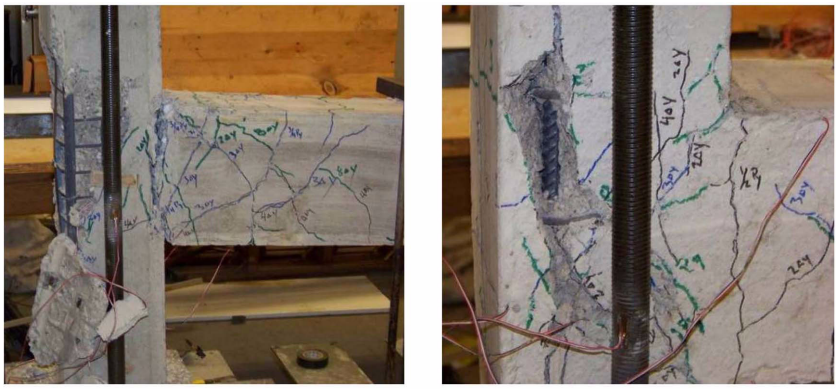

(a) (b)

Fig. 7 Specimens (a) C-2-PCS and (b) C-2-RC at the end of experiments

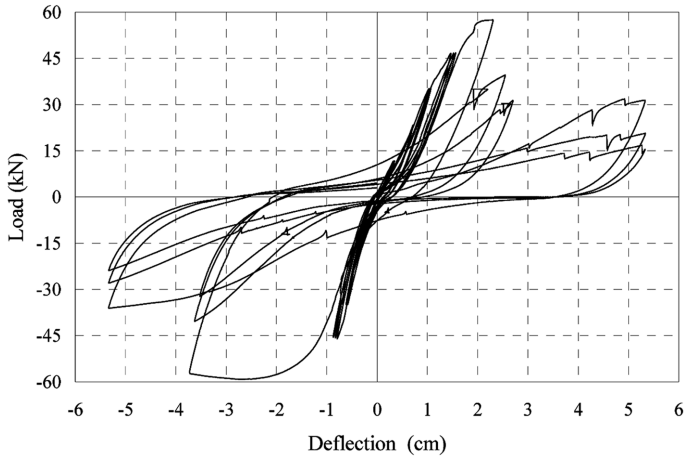

Fig. 8 Measured load versus deflection response for E-1-PCS

4.1 Group E specimens

Specimens within Group E (specimens E-1-PCS and E-1-RC) were able to withstand large deformations and maintain their strength beyond the yield strength of the beam. No visible cracking occurred during the first two loading cycles. During the $¾P_y$ load cycles, diagonal cracks began to form in the beam as well as within the joint region and vertical cracks began to form at the beam-column interface. During yield loading cycles, cover concrete over the joint region began spalling off. The cracks along the back of the column grew and cover concrete began to separate from the back of the column. During the $2\Delta_y$ cycles, the joint reached its maximum load capacity of 56.5 kN. During the following cycles, the strength and stiffness of the joint decreased significantly. The applied load and the corresponding displacement at the tip of the beam were monitored during the tests. The measured load-deflection response for E-1-PCS (Fig. 8) shows nearly linear-elastic joint behavior until the P_y cycle, at which point the first yielding occurred. After yielding, the joint

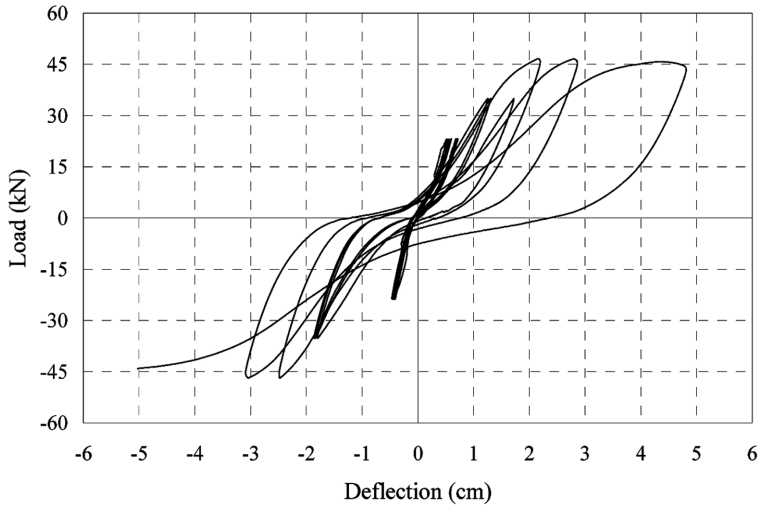

Fig. 9 Load versus deflection response for E-1-RC

capacity decreased while the deflection increased due to several factors: 1) concrete cracking and deterioration within the joint region, 2) steel softening after yielding, and 3) slipping of the beam reinforcement inside of the joint due to concrete deterioration. This large strength decrease first occurred after the joint reached a deflection of -35.6 mm and is observed during the following positive deflection cycle.

Small diagonal cracks formed in the joint region of specimen E-1-RC during the $\frac{1}{2}P_y$ load cycles. During the $\frac{3}{4}P_y$ cycle, shear cracks in the beam and joint began to widen up to 5 mm. Cover concrete around the joint region began to spall off. The joint reached its maximum load carrying capacity of 57.4 kN during the P_y cycles when failure occurred within the joint. The measured load-deflection response for Specimen E-1-RC is shown in Fig. 9. The observed response of E-1-RC leads to the conclusion that the specimen experienced shear-flexural failure within the joint region after the column longitudinal reinforcement yielded.

4.2 Group C specimens

Specimens within Group C were designed according to the seismic requirements of the ACI 318 code (2005). A hairline vertical crack formed at the beam-column interface of specimen C-2-PCS during the $\frac{3}{4}P_y$ load cycles. During the $2\Delta_y$ and $3\Delta_y$ cycles, additional diagonal and vertical cracks developed within the beam, as well as very fine diagonal cracks within the joint. During the $4\Delta_y$ cycles, vertical cracks at the beam-column interface began to widen significantly, up to 6 mm, and the joint reached its maximum load capacity of 54.3 kN (Fig. 10). Large diagonal cracks began to form within the joint region during the $6\Delta_y$ cycles. During the $8\Delta_y$ cycle, a clear separation formed at the interface between the beam and column. Testing was stopped after this cycle due to a significant loss of joint strength, which at the end of the cycle was 38% less than its maximum.

Little noticeable cracking occurred before the P_y cycles in specimen C-2-RC. During the P_y cycles, the crack at the beam-column interface began to widen. A combination of vertical and diagonal cracks began to form within the beam away from the joint. During the $2\Delta_y$ and $3\Delta_y$ cycles,

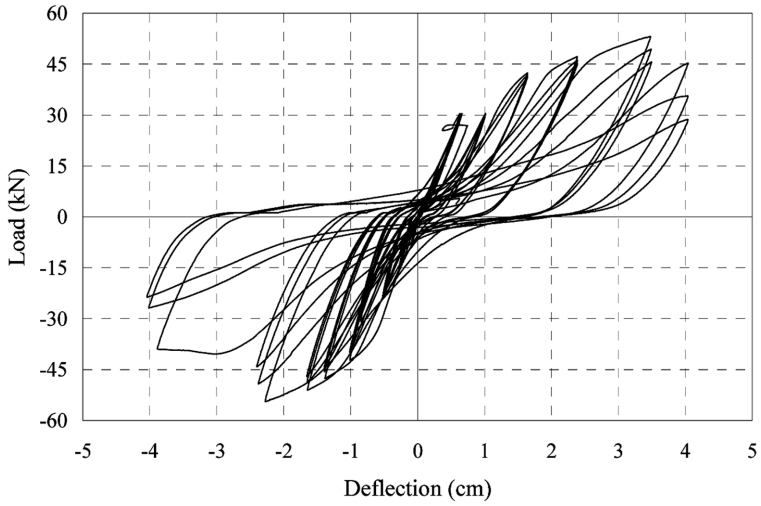

Fig. 10 Load versus deflection response for C-2-PCS

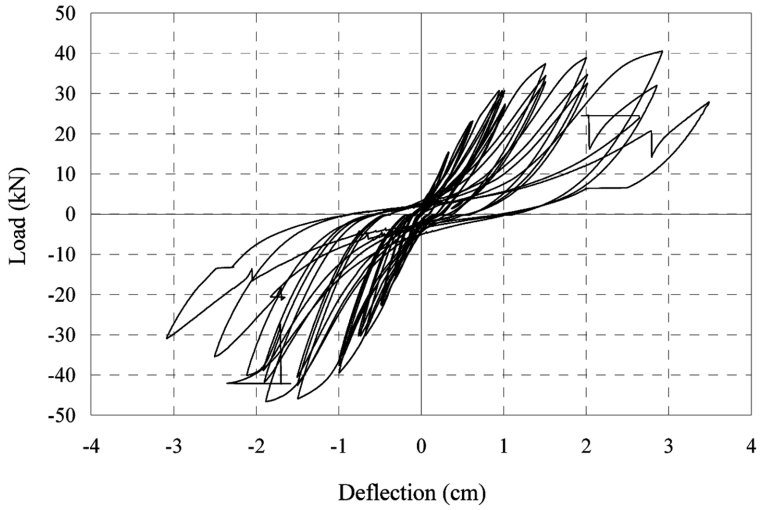

Fig. 11 Load versus deflection response for C-2-RC

the cracks within the joint continued to grow and. During the $4\Delta_y$ cycles, the vertical crack at the beam-column interface widened significantly. The number, length and width of cracks within the joint region increased and some cover concrete began to spall off during this cycle. A large amount of spalling occurred within the joint region. As shown in Fig. 11, a maximum load of 40.0 kN was carried by the specimen during the $6\Delta_y$ load cycles. Testing was later stopped due to significant loss of joint load carrying capacity, which was 33% less than the maximum capacity at the end of the last cycle.

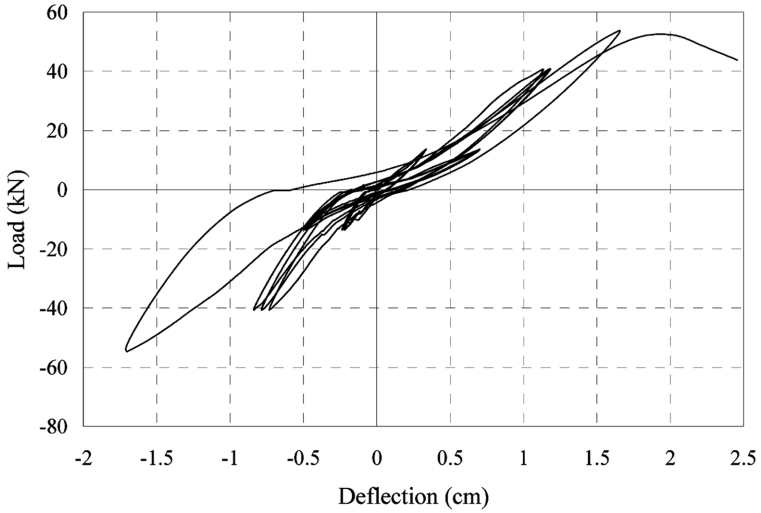

Fig. 12 Load versus deflection response for B-1-PCS

4.3 Group B specimens

During the $¾P_y$ loading cycles, diagonal and vertical cracks began to form in the beam, and diagonal cracks formed within the joint region of specimen B-1-PCS. A vertical crack also developed in the back of the column near the base during this loading cycle. During the P_y load cycles, a shear failure occurred within the cantilever beam. The measured load-deflection response for B-1-PCS is shown in Fig. 12.

During the $¾P_y$ cycles, diagonal and vertical cracks formed in the beam and diagonal cracks formed in the joint region of specimen B-1-RC. During the first P_y cycle, larger diagonal cracks developed in the joint region. Cover concrete began to spall off. The joint failed near the end of this cycle (Fig. 13). The majority of the damage was concentrated within the joint region, as was expected.

5. Comparison of results

The behavior of the specimens was sensitive to a number of factors including the amount of longitudinal steel in the beam, confinement of the joint concrete and yield strength of the longitudinal steel in the column. A comparison of the measured and predicted strengths of each specimen is presented in Table 2. Eq. (2) and specified material properties were used to calculate the joint shear strengths shown in Table 2. With the exception of specimens C-2-PCS and E-2-PCS, the maximum joint strength was predicted reasonably well.

The design of all columns was identical while the beams in each group had different amounts of longitudinal steel. Table 2 shows that the predicted strength of specimens increased along with beam strength. This is based on the assumption that the beam reaches its flexural strength and longitudinal steel yields at the beam-column interface. The controlling parameter for failure is the strength of

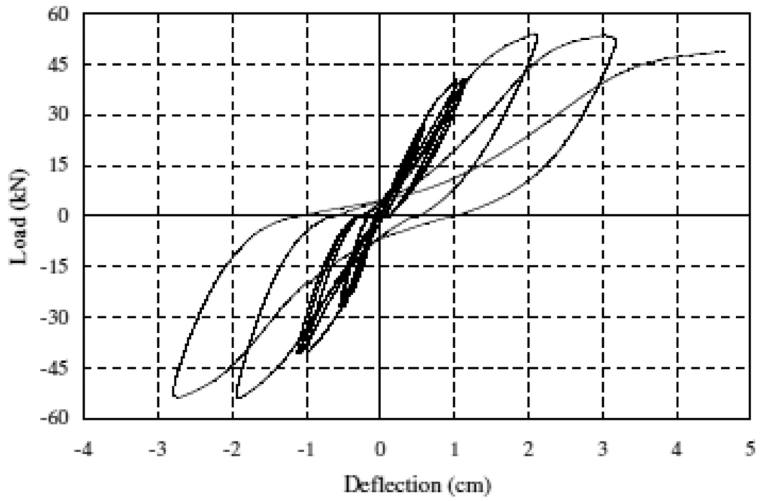

Fig. 13 Measured load versus beam deflection relationship for B-1-RC

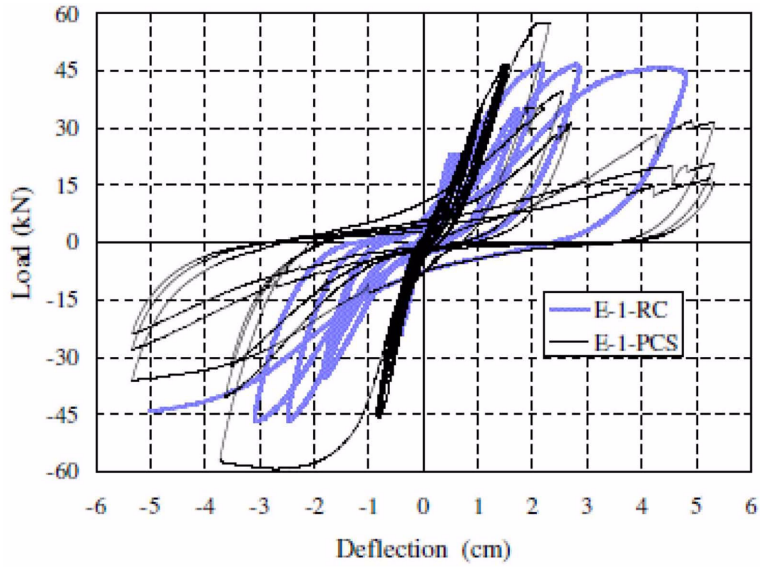

Fig. 14 Comparison of load-deflection responses for group E specimens

beam or joint region depending on when, where and how the damage starts and progresses. For these three unique joint designs, the objective was to compare the performance of rebar and PCS reinforced specimens. Consistent with the calculated beam flexural strength M_{nb}, tensile force in the beam longitudinal reinforcement T_n, total shear force resisted by the joint V_u, and shear strength of the joint ϕV_n, as reported in Table 1, beam longitudinal bars in all specimens yielded in all test specimens.

Table 2 Comparison of predicted versus actual shear strength of joints

Group	Specimen	Ultimate strength			% greater than predicted
		Predicted (kN)	Measured (+) (kN)	Measured (-) (kN)	
C	C-2-RC	39.6	40.5	-42.3	6.7%
	C-2-PCS		53.4	-54.3	37.1%
E	E-1-RC	48.0	46.7	-46.7	-2.8%
	E-1-PCS		57.4	-59.2	23.1%
B	B-1-RC	56.0	53.8	-53.8	-4.0%
	B-1-PCS		54.3	-54.7	-2.4%

5.1 Behavior of specimens in group E

The specimens in Group E (E-1-RC and E-1-PCS) were designed as Type 1 joints according to non-seismic or general joint design requirements found in ACI 318 code (2005) and ASCE-ACI 352R document (2002). E-1-PCS developed a hinge at the beam-column interface and ultimately failed due to deterioration of the concrete inside the joint. Comparison of load-deflection responses of specimens in Group E shows that E-1-PCS was significantly stronger than E-1-RC (Fig. 14). E-1-RC reached its maximum strength of 46.7 kN at a deflection of 48 mm. This result is nearly equal to the calculated design load of 48.0 kN (Table 2). At a deflection of 36 mm, E-1-PCS reached its maximum strength of 59.2 kN, which is 23% larger than the design strength (Table 2). The measured and observed performance of E-1-RC and E-1-PCS shows that the damage and deterioration are concentrated more inside the joint than inside the beam. The larger strength and deflection capacity of E-1-PCS suggests that the PCS reinforcement provides better confinement for the joint concrete and delays its deterioration and crushing.

5.2 Behavior of specimens in group C

In both specimens in Group C, large cracks formed at the beam-column interface, followed by deterioration of concrete inside the joint and slippage of the beam reinforcement anchored within the joint. Measured load-deflection responses shown in Fig. 15 show that C-2-PCS had larger deformation capacity and was significantly stronger than C-2-RC in both loading directions. For C-2-RC, the maximum load reached was 42.3 kN at a deflection of 31 mm. This strength is slightly greater than the calculated shear design load of 39.6 kN. C-2-PCS reached a maximum strength of 54.3 kN, also at a deflection of 31 mm. Fig. 15 shows that the strength of C-2-RC started degrading at about 31 mm deflection, however C-2-PCS was able to maintain a larger strength capacity at a maximum deflection of 41 mm. The maximum load capacity of C-2-PCS exceeded that of C-2-RC by 12.0 kN, or 28%. The material properties and design details were nominally identical in both specimens in this group. No unexpected problems occurred during testing of either specimen that could account for the disparity between the results. Experimental data suggest that PCS reinforcement within the column of C-2-PCS provided a stronger and more ductile joint than the rebar reinforcement in C-2-RC.

5.3 Behavior of specimens in group B

The specimens in Group B were designed as Type 1 or non-seismic joints. B-1-RC ultimately experienced shear failure within the joint. B-1-PCS ultimately experienced shear failure in the beam. Comparison of the responses of each specimen shown in Fig. 16 indicates that both specimens had almost equal strengths, 53.8 kN for B-1-RC and 54.7 kN for B-1-PCS, which were both slightly less than the design strength of 56 kN (Table 2). Fig. 16 shows that B-1-RC has greater deformation capacity than B-1-PCS. However, up until the shear failure in the beam, the joint region in B-1-PCS had suffered little damage as evidenced by the load-deflection response in Fig. 16 as well as visual inspection during testing. Based on their intentional poor seismic design, the specimens in Group B were expected to behave in a brittle manner. The design intent of this group was to force failure into the column portion of the joint region. While this is neither a typical design nor a good or practical design, it was used in this research to compare the performance of joints with substandard details commonly found in existing buildings.

5.4 Performance of PCS specimens

While it is not possible to directly compare the response of three PCS specimens due to their varying designs, it is possible to compare how each specimen performed in relation to the equivalent rebar reinforced specimen in each group. Of the three specimens, C-2-PCS exceeded its expected capacity by the largest margin. The maximum load capacity of C-2-PCS was 37% greater than its design strength. E-1-PCS also performed significantly better than expected, exceeding its design strength by 23%. The performance evaluation of B-1-PCS was difficult because the failure occurred in the beam instead of within the joint region. PCS has been shown to provide better confinement ability and allow for greater ductility in beam-column joints. E-1-PCS and B-1-PCS were both designed with very little or no joint ductility and did not perform as well as C-2-PCS. C-2-PCS was designed as a Type 2 seismic joint, in which joint ductility was a necessity. This PCS reinforced joint was able to sustain greater deformations and maximum load than the equivalent rebar reinforced joint specimen.

6. Conclusions

One objective of this study was to provide insight into the potential of PCS reinforcement used in an exterior beam-column joint. Overall, joints reinforced with PCS performed as well or better than the similar rebar reinforced joints. The strength of the PCS member in Group C, with specimens designed according to seismic requirements, exceeded that of the equivalent rebar specimen by 36%. The strength of the PCS member in Group E, with non-seismic details, exceeded that of the equivalent rebar specimen by 23%. The PCS specimen in Group B was only able to match the maximum load capacity of the equivalent rebar specimen. In general, PCS reinforced specimens displayed good confinement ability, as evidenced by the lack of damage sustained within the joint compared to equivalent rebar reinforced specimens. PCS specimens were able to meet, and in two cases exceed significantly, the design strength required by the ACI 318 Building Code (2005) and ASCE-ACI 352 report (2002). The overall deformation ductility of the PCS members was slightly greater than the rebar equivalent.

The maximum strength of each of the three rebar reinforced specimens was within 7% of the design strength. As expected, C-2-RC developed a plastic hinge at the end of the beam, as evidenced by damage to the specimen being limited to outside of the joint region at failure. Specimens E-1-RC and B-1-RC underperformed significantly compared to the PCS equivalent. These two specimens sustained significant damage inside the joint region because these specimens did not meet the special seismic design requirements.

Comparison of measured load-displacement response of test specimens shows that the maximum displacement capacity of specimens in Group E was comparable (Fig. 14). The displacement capacity of C-2-RC was better than that of C-2-PCS (Fig. 15), while the maximum displacements observed in B-1-PCS were much larger than in B-1-RC (Fig. 16).

References

ACI Committee 318 (2008), "Building code requirements for structural concrete (ACI 318-05) and commentary (ACI 318R-05)," American Concrete Institute, Farmington Hills, MI.

ACI-ASCE Committee 352 (2002), "Recommendation for design of beam-column joints in monolithic reinforced concrete structures (ACI 352R-02)," American Concrete Institute, Farmington Hills, MI.

Alemdar, F. and Sezen, H. (2010), "Shear behavior of exterior reinforced concrete beam-column joints", *Struct. Eng. Mech.*, **35**(1), 123-126.

Bai, Y., Nie, J. and Cai, C.S. (2008), "New connection system for confined concrete columns and beams. ii: Theoretical Modeling", *ASCE J. Struct. Eng.*, **134**(12), 1800-1809.

Bakir, P.G. (2003), "Seismic resistance and mechanical behaviour of exterior beam-column joints with crossed inclined bars", *Struct. Eng. Mech.*, **16**(4), 493-517.

Bakir, P.G. and Boduroglu, H.M. (2002), "A new design equation for predicting the joint shear strength of monotonically loaded exterior beam-column joints", *Eng. Struct.*, **24**, 1105-1117.

Bindhu, K.R., Jaya, K.P. and Manicka, S.V.K. (2008), "Seismic resistance of exterior beam-column joints with non-conventional confinement reinforcement detailing", *Struct. Eng. Mech.*, **30**(5), 733-761.

Dogangun, A. (2004), "Performance of reinforced concrete buildings during the may 1 2003 bingol earthquake in Turkey", *Eng. Struct.*, **26**(6), 841-856.

Fisher, M. (2009), "Experimental evaluation of reinforcement methods for concrete beam-column joints", M.S. Thesis, Ohio State University.

Gencoglu, M. (2007), "The effect of stirrups and the extends of regions used SFRC in exterior beam-column joints", *Struct. Eng. Mech.*, **27**(2), 223-241.

Jiuru, T., Hu, C., Yang, K. and Yan, Y. (1992), "Seismic behavior and shear strength of framed joint using steel-fiber reinforced concrete", *ASCE J. Struct. Eng.*, **118**(2), 341-458.

Lee, J.Y., Kim, J.Y. and Oh, G.J. (2009), "Strength deterioration of reinforced concrete beam-column joints subjected to cyclic loading", *Eng. Struct.*, **31**, 2070-2085.

Qu, H., Han, L.H. and Tao, Z. (2009), "Seismic performance of reinforced concrete beam to concrete-filled steel tubular columns joints", *Key Eng. Mater.*, V. 400-402, 685-691.

Sezen, H. and Miller, E.A. (2011), "Experimental evaluation of axial behavior of strengthened circular reinforced concrete columns", *ASCE J. Bridge Eng.*, **16**(2), 238-247.

Sezen, H. and Shamsai, M. (2008), "High-strength concrete columns reinforced with prefabricated cage system", *ASCE J. Struct. Eng.,* **134**(5), 750-757.

Sezen, H., Whittaker, A.S., Elwood, K.J. and Mosalam, K.M. (2003), "Performance of reinforced concrete and wall buildings during the August 17, 1999 Kocaeli, Turkey earthquake, and seismic design and construction practice in Turkey", *Eng. Struct.*, **25**(1), 103-114.

Shamsai, M. (2006), "Prefabricated cage system for reinforcing concrete members", Ph.D. Dissertation, Ohio State University, Ohio.

Shamsai, M., Whitlatch, E. and Sezen, H. (2007), "Economic evaluation of reinforced concrete structures with

columns reinforced with prefabricated cage system", *ASCE J. Constr. Eng. Manage.*, **133**(11), 864-870.
Shamsai, M. and Sezen, H. (2011), "Behavior of square concrete columns reinforced with prefabricated cage system", *Mater. Struct.*, **44**, 89-100.
Shannag, M.J., Abu-Dyya, N. and Abu-Farsakh, G. (2005), "Lateral load response of high performance fiber reinforced concrete beam-column joints", *Constr. Build. Mater.*, **19**, 500-508.
Zhao, B., Taucer, F. and Rossetto, T. (2008), "Field investigation on the performance of building structures during the 12 May 2008 Wenchuan earthquake in China", *Eng. Struct.*, **31**, 1707-1723.